International Journal of Refrigeration 100 (2019) 434–442

Contents lists available at ScienceDirect

International Journal of Refrigeration

journal homepage: www.elsevier.com/locate/ijrefrig

Validation of multitask artificial neural networks to model desiccant wheels activated at low temperature

F. Comino[a,*], D. Guijo-Rubio[b], M. Ruiz de Adana[a], C. Hervás-Martínez[b]

[a] Departamento de Química-Física y Termodinámica Aplicada, Universidad de Córdoba, Córdoba, Spain
[b] Departamento de Informática y Análisis Numérico, Universidad de Córdoba, Córdoba, Spain

ARTICLE INFO

Article history:
Received 27 October 2018
Revised 30 January 2019
Accepted 1 February 2019
Available online 7 February 2019

Keywords:
Artificial neural networks
Sigmoid units
Empirical models for desiccant wheels

ABSTRACT

Desiccant wheels (DW) could be a serious alternative to conventional dehumidification systems based on direct expansion units, which depend on electrical energy. The main objective of this work was to evaluate the use of multitask artificial neural networks (ANNs) as a modelling technique for DWs activated at low temperature with low computational load and good accuracy. Two different ANN models were developed to predict two output variables: outlet process air temperature and humidity ratio. The results show that a sigmoid unit neural network obtained 0.390 and 2.987 for MSE and SEP, respectively. These results outline the effective transfer mechanism of multitask ANNs to extract common features of multiple tasks, being useful for modelling a DW activated at low temperature. On the other hand, moisture removal capacity of the DW and its performance were analysed under several inlet air conditions, showing an increase under process air conditions close to saturation air.

Validation de réseaux de neurones artificiels multitâches pour modéliser des roues déshydratantes activées à basse température

Mots-clés: Réseaux neuronaux artificiels; Unités sigmoïdes; Modèles empiriques de roues déshydratantes

1. Introduction

Dehumidification systems are necessary to maintain the required indoor conditions in buildings with high latent loads. Food and pharmaceutical industries also have a significant interest in controlling the internal moisture content, (De Antonellis et al., 2016; Wang et al., 2018). Excessive indoor air humidity can cause problems related to the indoor air quality of the building owing to moulds and fungus, (Bornehag et al., 2001). Therefore, it is necessary to control the humidity in an indoor environment.

Several techniques for removing moisture from air under ambient pressure conditions have been studied, (Mazzei et al., 2005). A widely used method to dehumidify air is the use of conventional dehumidification systems based on direct expansion units, i.e. DX systems, which operate according to the vapour-compression cycle. However, these units depend mainly on electrical energy. Desiccant dehumidification systems offer a promising alternative to conventional dehumidification units.

A type of desiccant dehumidification system is a desiccant wheel (DW). Many authors have analysed DWs experimentally and numerically (Cao et al., 2014; De Antonellis and Kim, 2018), in particular, focusing on the analysis of parameters influencing outlet process air conditions. The air regeneration temperature is usually used to control the outlet air conditions of DW (Harriman III, 2001), because the higher the regeneration air temperature, the higher is the dehumidification capacity. Nevertheless, significant energy consumption is required to achieve high regeneration temperature. Other studies showed an acceptable dehumidification capacity when the DW was activated at low temperature (Al-Alili et al., 2014; Comino et al., 2016; White et al., 2011), thus reducing the environmental impact associated with air dehumidification. In this study, values below 60 °C were considered as low regeneration temperatures.

* Corresponding author.
E-mail address: francisco.comino@uco.es (F. Comino).

https://doi.org/10.1016/j.ijrefrig.2019.02.002

Acronyms

ANN	artificial neural network
DCOP	dehumidification coefficient of performance
DW	desiccant wheel
HVAC	heating, ventilation, and air conditioning
m	number of nodes in the hidden layer
MRC	moisture removal capacity [$kg\,h^{-1}$]
n	size of the dataset
n_g	size of the generalisation dataset
P	pressure [Pa]
r	number of outputs
SEP	standard error of prediction
T	temperature [°C]
x	vector of inputs
#conn	number of connections of an ANN

Greek letters

Δ	increase
Ω	specific mass airflow rate [$kg\,s^{-1}\,m^{-3}$]

Subscripts

d	dewpoint
i	inlet
p	process
vs	vaporisation of water

Superscripts

$\bar{}$	mean value
Cp	specific heat of the air [$kJ\,kg^{-1}\,K^{-1}$]
d	number of inputs
h	enthalpy
L	loss function
$\dot{m}$	air mass flow rate [$kg\,h^{-1}$]
MSE	mean squared error
n_t	size of the training dataset
N	rotation speed [rph]
PUNN	product unit neural network
SD	standard deviation
SUNN	sigmoid unit neural network
$\dot{V}$	volumetric airflow rate [$m^3\,h^{-1}$]
y	vector of outputs
ω	humidity ratio [$g\,kg^{-1}$]
hc	heating coil
o	outlet
r	regeneration
$\wedge$	estimated output variable

Mathematical models of DWs can be very useful to optimise the device and study its annual behaviour when combined with other HVAC elements. Some authors developed detailed DW mathematical models, based on the heat and mass transfer in a DW (Ruivo et al., 2007). However, some physical characteristics and specific parameters of DWs are not available. Moreover, these models involve complex equations and assumptions, and hence, they are not easy to implement in energy simulation tools.

The use of simplified models of DWs is another mathematical modelling approach and it requires low computation load. A widely used simplified approach to study DWs is the model developed by Maclaine-Cross and Banks (1972), which is based on the effectiveness concept. However, high deviations can be obtained for wide ranges of input conditions (Ruivo et al., 2013). Other authors developed empirical simplified DW models based on correlations, adjusting the behaviour of the wheel with first- or second-order equations (Beccali et al., 2003; Comino et al., 2016). Besides, Zendehboudi and Li (2018) developed a multi-objective genetic algorithm combined with response surface methodology to optimise the process outlet air conditions of a DW.

Another approach is the technique of artificial neural network (ANN) (Bishop, 1995), which is widely used in engineering processes, due to their accuracy, versatility and ability to model multivariate complex and nonlinear systems, hence it has been hugely applied to solid desiccant systems (Jani et al., 2017). Previous works studied the behaviour of a DW using ANN models (Koronaki et al., 2012; Yang et al., 2017). However, the ANNs used required a high number of connections and were difficult to interpret. Other proposals of modelling DWs using ANN were trained with back-propagation algorithms (Jani et al., 2016; Parmar and Hindoliya, 2011; Uçkan et al., 2015). Nevertheless, they usually do not find the global minimum of the error function. Furthermore, these works focused their study on DW activated at high temperatures, using small ranges of experimental validity and without including a mathematical model of DW.

Based on the limitations of previous works, it would be interesting to obtain a robust and easy-to-interpret model of DW using multitask neural network models, which allow predicting several outputs simultaneously in a single model, with many fewer connections between nodes and low complexity compared to the works already done. Besides, a DW model valid for low regeneration temperatures, which can be combined with low temperature heating sources, such as waste energy from refrigeration facilities or low temperature renewable energies. Other novelty of the work would be the use of ANN trained with genetic algorithms, which, in general, find the global minimum of the error function with more probability than gradient methods, whereas the previous works on modelling DW proposed feed-forward neural networks combined with back-propagation algorithms. Summarizing, genetic algorithms obtain better solutions than other gradient-based algorithms such as back-propagation. Furthermore, product unit neural networks have not been studied in previous works, due to the need for training them with genetic algorithms.

The main objective of this work was to apply ANN technique to develop an empirical parsimonious model of a DW activated at low temperature with low computational load and good accuracy. Therefore, numerous experimental tests were performed by modifying the inlet air temperatures, humidity ratios and air flow rates of the DW. A secondary objective was to analyse the influence of the inlet process and regeneration air conditions on the moisture removal capacity of the DW and its performance.

2. Methodology

2.1. Experimental setup and data

An experimental test facility was used to study the thermal behaviour of a DW under different working conditions. A layout of the test facility is shown in Fig. 1. The facility was designed with a counter-current arrangement between two air streams through the DW: process air and regeneration air. The inlet temperature and humidity ratio of both process and regeneration streams were set using two air handling units, AHU, which were composed of a heating coil, an electric heater, a cooling coil and a steam humidifier, located, for each air stream, upstream of the DW. Both airflow rates were set with variable speed fans. These HVAC elements were controlled by two CAREL systems, model pCO3Medium, which allowed to manage the AHUs by means of a programmable controller. A detailed description of the test facility and the technical characteristics of the different HVAC elements were reported in a previous work of the authors (Comino et al., 2016).

An image of the DW of the test facility is shown in Fig. 2. The technical data of the DW are presented in Table 1.

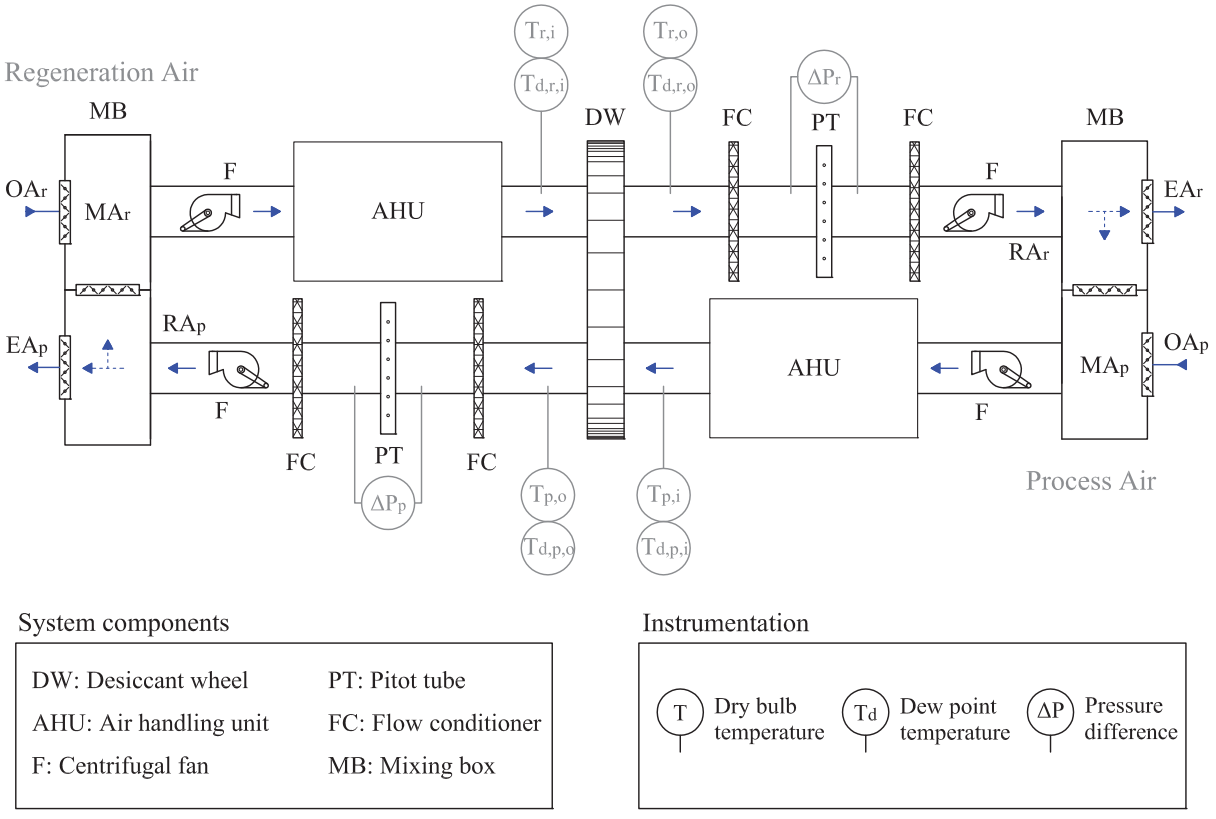

Fig. 1. Layout of the experimental test facility.

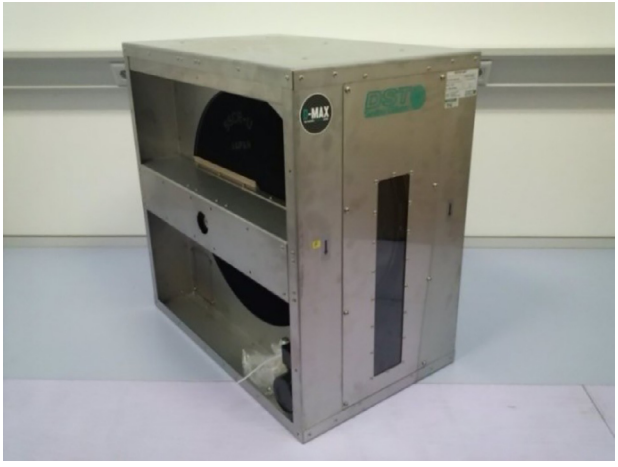

Fig. 2. Image of the DW.

Table 1
Technical data of the DW.

Parameters	Value	
Nominal capacity	15	[kg h^{-1}]
Nominal air flow	2300	[m^{3}h^{-1}]
Rotor diameter	500	[mm]
Rotor thickness	200	[mm]
Nominal rotation	42	[rph]
Weight	57	[kg]
Ratio	1/1	
Material	Silica gel	

Table 2
Specifications of measuring instruments.

Measured parameter	Type	Accuracy
$T_{p,i}$, $T_{p,o}$, $T_{r,i}$, $T_{r,o}$	PT100	±0.12 °C
$T_{d,p,i}$, $T_{d,p,o}$	Chilled mirror hygrometer	±0.15 °C
$T_{d,r,i}$, $T_{d,r,o}$	Capacitive	±0.4 °C
ΔP_p, ΔP_r	Differential pressure transmitter	±0.3 % (0 to 1 mbar)

The dry bulb temperature and dew point temperature were measured at the input and output of the DW. The specifications of the measuring devices in the test facility are listed in Table 2. In each experimental session, at least 400 samples with sampling time steps of 3 s of each physical quantity were obtained under steady-state conditions.

These experimental tests covered a wide range of operating conditions of the process and regeneration air flows, as shown in Fig. 3. The values of the working ranges for the process and regeneration air streams are shown in Table 3.

Finally, a total of 192 experimental tests were performed in this study. All the experimental tests are listed in supplementary material. They were divided into two parts: first, a 60% for the training dataset (test N1 to test N115) in order to train the ANN models and second, the remaining 40% for prediction dataset (test N116 to test N192) in order to generalise the model developed.

2.2. ANN models

In this study, the prediction of two real-valued output variables ($T_{p,o}$ and $\omega_{p,o}$) were considered, this sort of prediction is known in machine learning as multitask learning.

To estimate a model, a set of samples is required for training the model (n_t), $(\mathbf{x}_i, \mathbf{y}_i)$, $i = 1 \dots n_t$, $\mathbf{x}_i \in \mathbb{R}^d$, $\mathbf{y}_i \in \mathbb{R}^2$, where d is the number of inputs. To solve this kind of problem, non-linear models were used. In this work, we focused on ANN models using

Table 3
Working ranges of the experimental tests of training data.

Ranges	Input variables						Output variables	
	$T_{p,i}$ [°C]	$\omega_{p,i}$ [g kg^{-1}]	$T_{r,i}$ [°C]	$\omega_{r,i}$ [g kg^{-1}]	Ω [kg s^{-1} m^{-3}]	N [rph]	$T_{p,o}$ [°C]	$\omega_{p,o}$ [g kg^{-1}]
Min	16.95	11.42	32.58	10.32	12.03	4.00	23.43	6.96
Max	30.06	24.85	52.06	30.35	33.47	41.00	39.21	21.36

Table 4
Parameters and values of the evolutionary algorithm and PUNN and SUNN models.

Evolutionary algorithm	
Runs	30
Generations	1000
Population size	1000
Hidden nodes to be created or deleted	[1, 2]
Minimum hidden nodes initialisation	1
Maximum hidden nodes initialisation	1
Maximum hidden nodes whole process	3
PUNN models	
Weights between input-hidden layer	[−1, 1]
Weights between hidden-output layer	[−5, 5]
SUNN models	
Weights between input-hidden layer	[−5, 5]
Weights between hidden-output layer	[−5, 5]

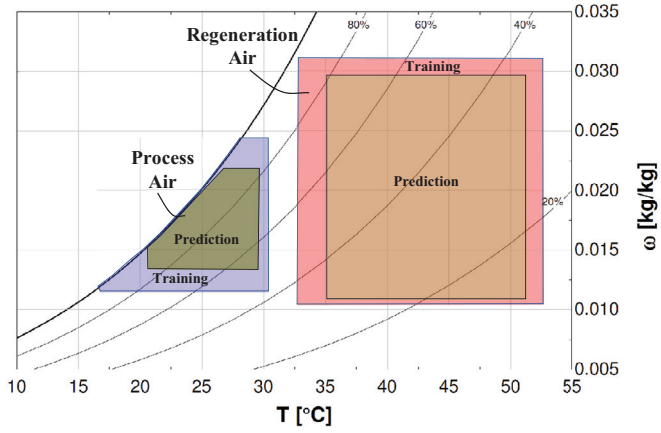

Fig. 3. Area considered for the inlet states of the process and regeneration airflow.

two different basis functions: product unit neural networks (PUNN) (Durbin and Rumelhart, 1989), and sigmoid unit neural network (SUNN) (Haykin, 2009). PUNN models provide high versatility for implementing high-order functions, retaining the properties of a universal approximator and using only a small number of neurons with multiplicative units instead of additives ones. On the other hand, SUNN models use sigmoid transfer functions for nodes of the hidden layer. This kind of neural network is most widely used owing to its ability to approximate any continuous function accurately. As PUNN and SUNN do not require a high number of neurons for solving certain problems (Hornik et al., 1989), thus, their application to this problem is reasonable.

From these basis functions, the ANN architecture was developed using evolutionary algorithms similar to those reported by Angeline et al. (1994), to estimate both the parameters and the architecture of the multitask neural networks proposed in this paper. Further details of this algorithm could be found in Angeline et al. (1994).

The parameters of the evolutionary algorithm are shown in Table 4. These values were selected by cross-validating them over the training set, and the other values were obtained from Martínez-Estudillo et al. (2006).

The methodology of the ANN was designed to fit several empirical models used to predict the outlet process air temperature, $T_{p,o}$, and the outlet process air humidity ratio, $\omega_{p,o}$, of the DW. Two different approaches were studied: first, the use of individual models that separately predict $T_{p,o}$ and $\omega_{p,o}$, and second, the use of models that predict both outputs using only one multitask ANN. This point of view follows the multitask paradigm, which has been successfully used across all applications of machine learning (Bishop, 1995). Both situations were studied using several input variables: inlet process air temperature, $T_{p,i}$, inlet process air humidity ratio, $\omega_{p,i}$, process specific mass airflow rate, Ω_p (ratio of inlet mass velocity to the channel length (Ruivo et al., 2013)), inlet regeneration air temperature, $T_{r,i}$, inlet regeneration air humidity ratio, $\omega_{r,i}$, regeneration specific mass airflow rate, Ω_r, and rotation speed, N. In both air streams, the same air flow rate values were employed for all cases in this study; thus, both specific mass airflow rates were denoted as Ω.

Prior to using these six inputs, they were scaled within the range [1, 2] for PUNN models, in order to prevent having input values close to zero, which produces large values in the case of negatives exponents. Moreover, the upper bound was chosen to avoid large changes in the outputs when the weights and exponents have a high value. Regarding SUNN models, the inputs were scaled to the range [0.1, 0.9] in order to avoid saturation problems in the sigmoidal basis function, where weights would be driven to infinite. Nevertheless, both outputs were scaled to the range [0, 1].

More information of the ANN methodology can be obtained from the papers (Mohammad et al., 2013; Zain et al., 2010), which include a wide explanation of the techniques proposed and its application to similar fields of the state of the art.

2.3. ANN evaluation

The accuracy of each model was evaluated in terms of MSE and standard error of prediction (SEP), which are widely used for regression problems. MSE is expressed by Eq. (1):

$$MSE = \frac{1}{r}\frac{1}{n}\sum_{k=1}^{r}\sum_{i=1}^{n}\left(y_i^k - \hat{y}_i^k\right)^2, \tag{1}$$

where r is the number of outputs, n is the size of the set (n_t for the training set and n_g for the generalisation set), and y_i^k and $\hat{y}_i^k$ are, respectively, the real and expected values of output k. Further, SEP is expressed by Eq. (2):

$$SEP = \frac{1}{r}\sum_{k=1}^{r}\frac{100}{|\bar{y}^k|}\sqrt{\frac{1}{n}\sum_{i=1}^{n}\left(y_i^k - \hat{y}_i^k\right)^2}, \tag{2}$$

where $\bar{y}^k$ is the mean value of output k for the training or the generalisation set, depending on the set evaluated.

2.4. Evaluation of the desiccant wheel

Modifications of the inlet air conditions in a DW cause variations in the outlet air conditions. The energy performance of the

Table 5
Values of *MSE*, *SEP*, and *#conn* obtained for DW problem using PUNN, SUNN, linear, and quadratic models.

$\hat{T}_{p,o}$						
	MSE		*SEP*		*#conn*	
	Mean ± SD	Best	Mean ± SD	Best	Mean ± SD	Best
SUNN (6,3,1)	0.621 ± 0.208	0.346	2.525 ± 0.416	1.911	20.63 ± 1.73	23
PUNN (6,3,1)	0.671 ± 0.062	0.547	2.657 ± 0.124	2.400	16.20 ± 1.69	16
Linear model	–	0.671	–	2.660	–	7
Quadratic model	–	0.353	–	1.930	–	28
$\hat{\omega}_{p,o}$						
	MSE		*SEP*		*#conn*	
	Mean ± SD	Best	Mean ± SD	Best	Mean ± SD	Best
SUNN (6,3,1)	0.292 ± 0.045	0.235	3.840 ± 0.287	3.454	19.93 ± 1.50	22
PUNN (6,3,1)	0.304 ± 0.042	0.253	3.921 ± 0.254	3.580	13.67 ± 3.80	17
Linear model	–	0.256	–	3.598	–	7
Quadratic model	–	0.257	–	3.607	–	28
$\hat{T}_{p,o}$ and $\hat{\omega}_{p,o}$						
	MSE		*SEP*		*#conn*	
	Mean ± SD	Best	Mean ± SD	Best	Mean ± SD	Best
SUNN (6,3,2)	0.621 ± 0.163	0.390	3.668 ± 0.362	2.987	24.83 ± 1.58	23
PUNN (6,3,2)	0.626 ± 0.200	0.407	3.622 ± 0.402	3.108	19.57 ± 1.59	21

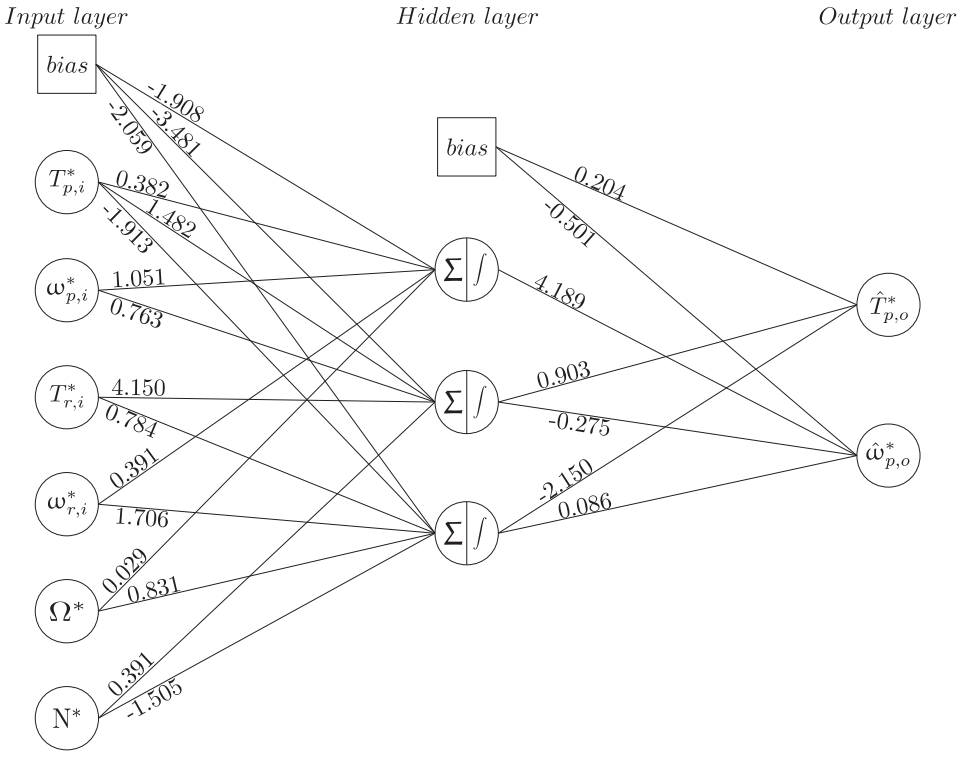

Fig. 4. The best model obtained, i.e. the SUNN model, for DW activated at low temperature.

DW activated at low temperature by setting the inlet air conditions was evaluated using the best ANN model, according to the following parameters:

- Moisture removal capacity (MRC) expressed by Eq. (3). ASHRAE defined MRC as a primary figure-of-merit for DW performance, ASHRAE (2007).

$$MRC = \dot{m}_{p,i} \cdot (\omega_{p,i} - \hat{\omega}_{p,o}) \tag{3}$$

- Dehumidification coefficient of performance (DCOP) expressed by Eq. (4). It represents the ratio of latent energy of the process air achieved with the DW and sensible energy delivered to thermally activate the DW.

$$DCOP = \frac{\dot{m}_p \cdot \Delta h_{vs} \cdot (\omega_{p,i} - \hat{\omega}_{p,o})}{\dot{m}_r \cdot C_p \cdot (T_{r,i} - T_{hc,i})}, \tag{4}$$

where $T_{hc,i}$ is the inlet air temperature to the heating coil, which is a constant value, and Δh_{vs} is the latent heat of vaporisation of water. It was calculated using the correlations provided by Angrisani et al. (2012), Eq. (5).

$$\begin{aligned}\Delta h_{vs} = &-0.614342 \cdot 10^{-4} \cdot T^3_{p,i} + 0.158927 \cdot 10^{-2} \cdot T^2_{p,i} \\ &-0.236418 \cdot 10 \cdot T_{p,i} + 0.250079 \cdot 10^4\end{aligned} \tag{5}$$

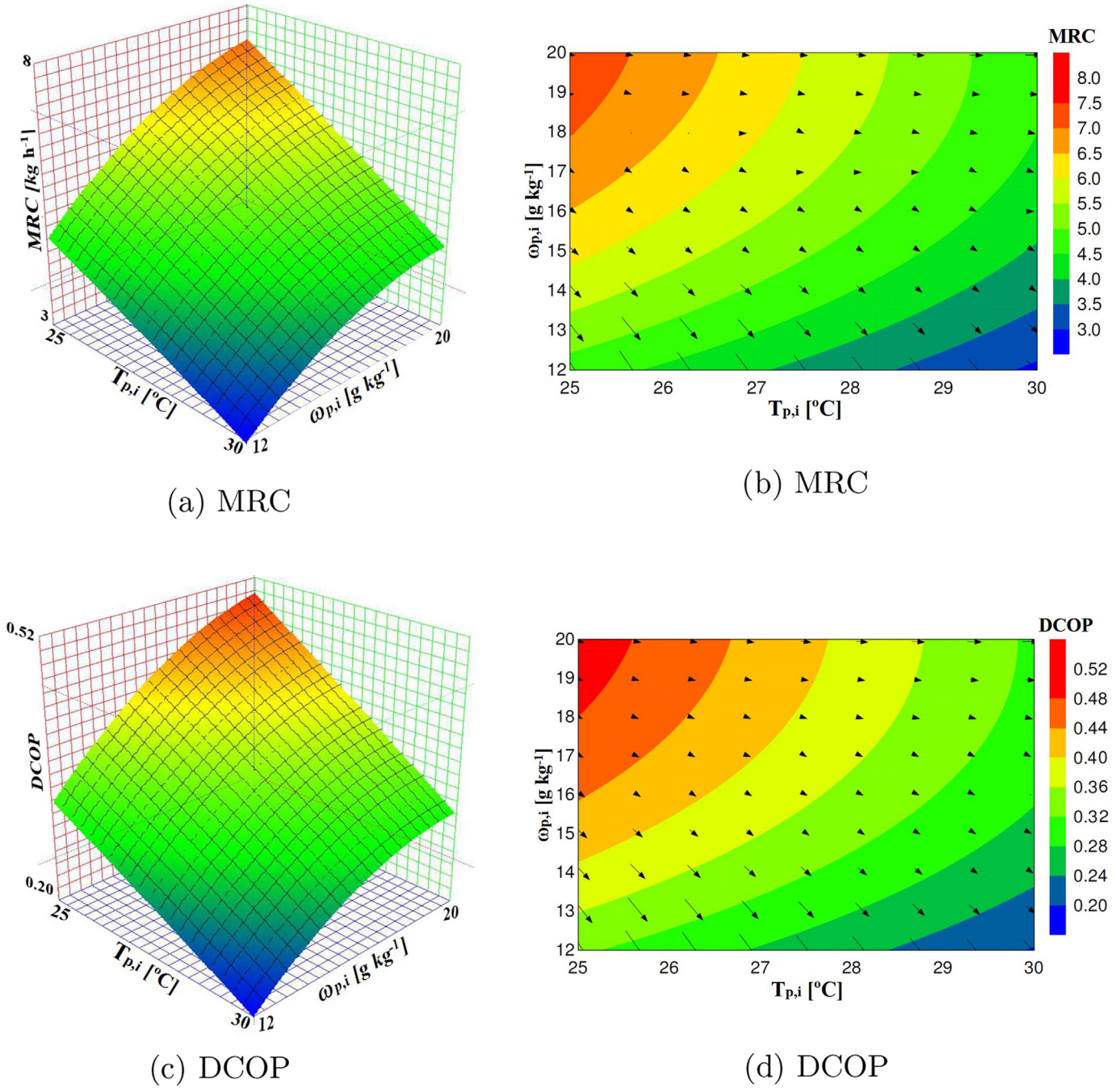

Fig. 5. Relationships between $T_{p,i}$ and $\omega_{p,i}$ for MRC, and DCOP.

3. Results and discussion

3.1. Experimental ANN models

To compare the predictive ability of PUNN and SUNN models in terms of architecture, number of connections, homogeneity, and accuracy, multitask models using six inputs and two outputs were designed. The results obtained for these models and a baseline comparison against linear, quadratic, PUNN, and SUNN models for each output are shown in Table 5. The architecture of each neural network is defined by using the following nomenclature (*d, m, r*), where *d* is the number of inputs, *m* is the number of hidden nodes, and *r* is the number of outputs of the model.

Table 5 is divided into three parts: (1) models that only predict $T_{p,o}$, (2) models predicting only $\omega_{p,o}$ as output, and (3) models with two nodes ($T_{p,o}$ and $\omega_{p,o}$) in the output layer. For all these models, the mean and standard deviation (SD) of the *MSE*, *SEP* and number of connections (*#conn*), and the corresponding values for the best model are shown. As these metrics measure the error incurred by the model, the main objective is to minimise them. It can be observed that most models provided satisfactory results.

Considering the characteristics of the problem, PUNN and SUNN models could achieve a better performance than other linear methods using fewer connections. The best results in terms of *MSE* and *SEP* were obtained by using two different models of SUNN, achieving the mean values 0.290 and 2.683, respectively, using 45

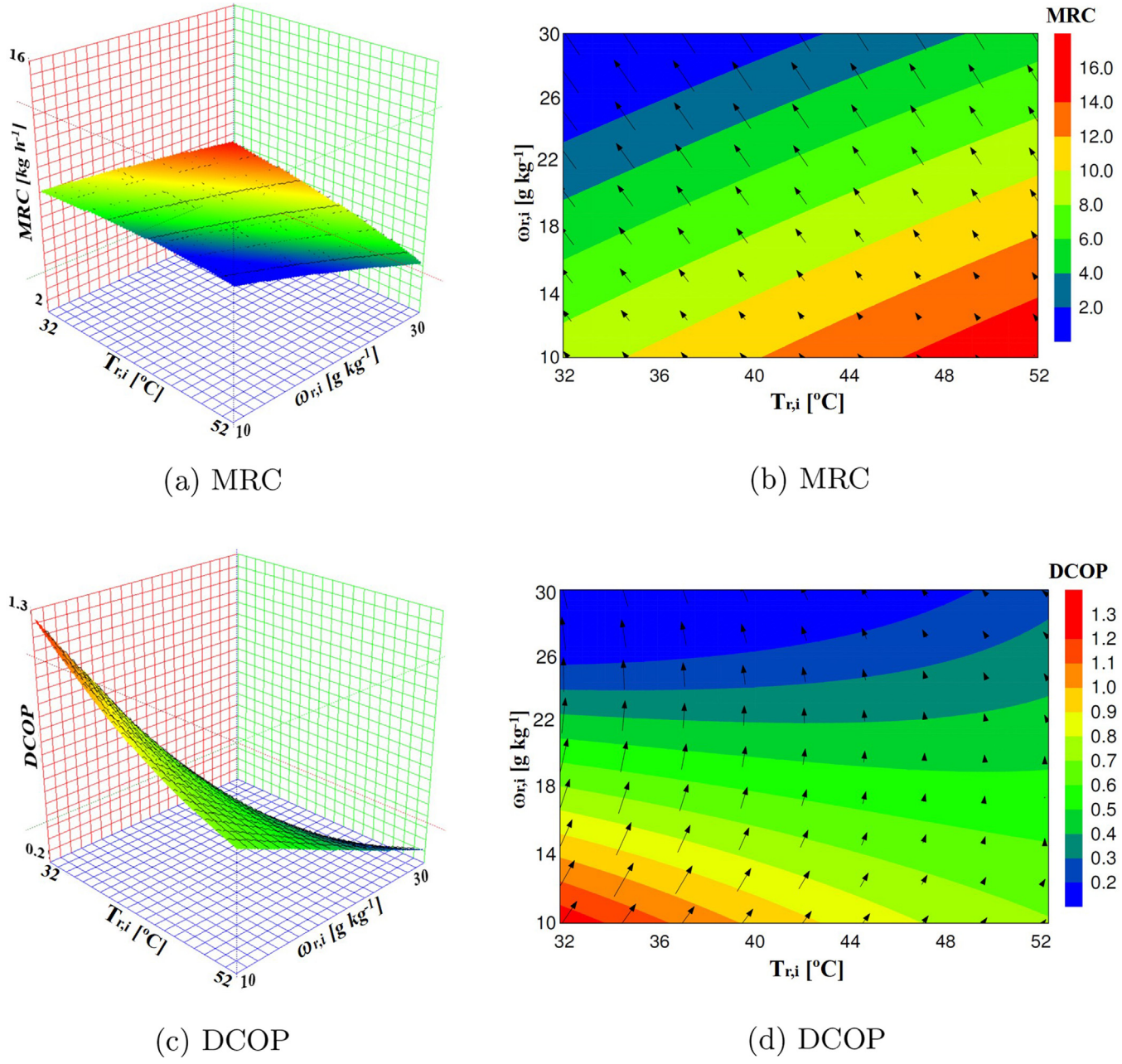

Fig. 6. Relationships between $T_{r,i}$ and $\omega_{r,i}$ for MRC, and DCOP.

connections. Although the best results were achieved by using these models, it was more interesting to approximate both outputs with only one multitask ANN. Multitask learning is an inductive transfer mechanism whose main goal is to improve the generalisation. Thus, it is believed that neural networks are convenient to extract common features of multiple tasks (Bengio et al., 2013). Thus, the model that best fitted both outputs ($T^*_{p,o}$ and $\omega^*_{p,o}$) while minimising *MSE* and *SEP* was the model that used SUNN as the basis function. This model achieved *MSE* of 0.390 and *SEP* of 2.987 by using only 23 connections, as shown in Table 5. The architecture of this best model for the two outputs was 6,3,2, see Fig. 4. Eqs. (6) and (7) show the output functions for $\hat{T}^*_{p,o}$ and $\hat{\omega}^*_{p,o}$ for SUNN model with both output variables, respectively. It can be observed that these output functions share two basis functions, which demonstrates the interrelation between $\hat{T}^*_{p,o}$ and $\hat{\omega}^*_{p,o}$.

$$\hat{T}^*_{p,o} = 0.204 + 0.903 \cdot B_2 - 2.150 \cdot B_3, \tag{6}$$

$$\hat{\omega}^*_{p,o} = -0.501 + 4.189 \cdot B_1 - 0.275 \cdot B_2 + 0.086 \cdot B_3, \tag{7}$$

where, B_1, B_2, and B_3 are defined as follows:

$$B_1 = \frac{1}{1 + e^{-(-1.908 + 0.382T^*_{p,i} + 1.051\omega^*_{p,i} + 0.391\omega^*_{r,i} + 0.029\Omega^*)}} \tag{8}$$

$$B_2 = \frac{1}{1 + e^{-(-3.481 + 1.482T^*_{p,i} + 0.763\omega^*_{p,i} + 4.150T^*_{r,i} + 0.391N^*)}} \tag{9}$$

$$B_3 = \frac{1}{1 + e^{-(-2.059 - 1.913T^*_{p,i} + 0.784T^*_{r,i} + 1.706\omega^*_{r,i} + 0.831\Omega^* - 1.505N^*}} \tag{10}$$

The remaining ANN, linear, and quadratic models obtained are shown in supplementary material.

The performance of the best ANN model is good and its application to the problem presented herein is interesting, owing to its

non-complex model, which exhibits a good performance. Approximating both outputs functions leads to a huge reduction in the error measures; moreover, owing to its fewer connections, it achieves more robust results.

3.2. Performance analysis of the desiccant wheel

The influence of the input variables on the outlet process air conditions in the DW activated at low temperature was obtained. These results are shown in supplementary material.

The energy performance of the DW activated at low temperature was studied using the two evaluation parameters: MRC and DCOP, given by Eqs. (3)–(5). The results of these parameters were obtained using the best ANN model, i.e. Eqs. (6)–(10). The relationships between the input variables and the two evaluation parameters are shown in Figs. 5 and 6.

The evaluation parameters were represented as a function of the input variables $T_{p,i}$ and $\omega_{p,i}$, as shown in Fig. 5. The remaining input variables were fixed at constant values: $T_{r,i} = 42.32\,^{\circ}\mathrm{C}$, $\omega_{r,i} = 20.34\,\mathrm{g\,kg^{-1}}$, $\Omega = 22.76\,\mathrm{kg\,s^{-1}\,m^{-3}}$, and $N = 41$ rph. These constant values correspond to the average values of the set of experimental tests. It can be observed that MRC values increased when $T_{p,i}$ decreased and $\omega_{p,i}$ remained constant (see Fig. 5a and b). MRC values also increased as $\omega_{p,i}$ was increased, when $T_{p,i}$ remained constant. The effects of interaction between both the input variables show that the maximum MRC value was $7.34\,\mathrm{kg\,h^{-1}}$, achieved with the minimum $T_{p,i}$ value, 25 °C, and the maximum $\omega_{p,i}$ value, $20\,\mathrm{g\,kg^{-1}}$.

The trends of DCOP with respect to the input variables $T_{p,i}$ and $\omega_{p,i}$ are shown in Fig. 5c and d. It can be observed that the DCOP values increased when $T_{p,i}$ was reduced, for constant $\omega_{p,i}$ values. The increase in the input variable $\omega_{p,i}$ also increased the DCOP values, when $T_{p,i}$ remained constant. The maximum DCOP value achieved by the DW was 0.5, obtained for the minimum $T_{p,i}$ values, 25 °C, and the maximum $\omega_{p,i}$ value, $20\,\mathrm{g\,kg^{-1}}$.

These results suggest that both the MRC and the DCOP of a DW increase when the process air conditions are close to the saturation conditions. These results are consistent with those obtained in previous studies (Kosar, 2006).

The relationships between $T_{r,i}$ and $\omega_{r,i}$ for the two evaluation parameters are presented in Fig. 6. The remaining input variables were fixed at constant values: $T_{p,i} = 24\,^{\circ}\mathrm{C}$, $\omega_{p,i} = 18\,\mathrm{g\,kg^{-1}}$, $\Omega = 22.76\,\mathrm{kg\,s^{-1}\,m^{-3}}$, and $N = 41$ rph. It can be observed that MRC increased when $T_{r,i}$ was increased and $\omega_{r,i}$ remained constant (see Fig. 6a and b). As $\omega_{r,i}$ was decreased, MRC values increased when $T_{r,i}$ remained constant. The effects of interaction between both the input variables show that the maximum MRC value was $15.59\,\mathrm{kg\,h^{-1}}$, achieved for the highest $T_{r,i}$ value, 52.5 °C, and the lowest $\omega_{r,i}$ value, $10\,\mathrm{g\,kg^{-1}}$ (see Fig. 6a and b).

Finally, the trends of DCOP are represented in Fig. 6c and d. It can be observed that the DCOP values increased after maintaining $T_{r,i}$ at a constant value and reducing $\omega_{r,i}$. This trend was obtained as the latent energy of the process air increased and the sensible energy delivered to thermally activate the DW remained constant (see Eq. (4)). However, three different trends of DCOP were obtained when $T_{r,i}$ was increased and $\omega_{r,i}$ remained constant (see Fig. 6c and d). For all three trends, the latent energy of the process air and sensible energy to thermally activate the DW increased, but in different proportions. First, for low $\omega_{r,i}$ values and an increase in $T_{r,i}$, the increase in the latent energy of the process air was greater than that of the sensible energy to thermally activate the DW (see Fig. 6d). Therefore, the highest DCOP value was achieved for the lowest $T_{r,i}$ values. Subsequently, for medium $\omega_{r,i}$ values, both the latent energy of the process air and the sensible energy to thermally activate the DW increased equally, and hence, the DCOP values remained constant. Finally, for high $\omega_{r,i}$ values and an increase in $T_{r,i}$, the increase in the latent energy of the process air was less than that of the sensible energy to thermally activate the DW (see Fig. 6d). Therefore, the highest DCOP value was obtained for the highest $T_{r,i}$ values.

The results indicated that, for low values of $T_{r,i}$ and $\omega_{r,i}$, the thermal activation heat helped mainly to remove the process moisture (see Fig. 6c and d). However, for low $T_{r,i}$ values and high $\omega_{r,i}$ values, the thermal activation heat was used mainly to increase the process air temperature.

4. Conclusions

This study evaluated the use of multitask ANNs as a modelling technique for DWs activated at low temperature, with low computational cost and good accuracy. Numerous experimental tests were performed under different inlet air conditions of a DW. Based on the results obtained, the following conclusions can be drawn:

1. The results obtained showed that the SUNN model with both output variables was the best method for modelling the DW, minimising its error of approximation. For this model, the values of MSE and SEP were 0.390 and 2.987, respectively, by using only 23 connections, thus demonstrating outstanding performance.
2. This best model was used to analyse the influence of MRC and DCOP of the DW on several inlet process and regeneration air conditions.
3. The results obtained showed that both MRC and DCOP values increased when the process air conditions were close to the saturation conditions.
4. Multitask ANN models have an effective transfer mechanism to extract common features of multiple tasks; thus, they are very useful for modelling a DW activated at low temperature.

Acknowledgment

This work has been subsidised by the projects with references TIN2017-85887-C2-1-P and TIN2017-90567-REDT of the Spanish Ministry of Economy and Competitiveness (MINECO) and FEDER funds. David Guijo-Rubio's research has been subsidised by the project PI15/01570 of the Fundación de Investigación Biomédica de Córdoba (FIBICO) and by the FPU Predoctoral Program (Spanish Ministry of Education and Science), grant reference FPU16/02128. The authors F. Comino and D. Guijo-Rubio contributed equally to the preparation of this paper.

Supplementary material

Supplementary material associated with this article can be found, in the online version, at doi:10.1016/j.ijrefrig.2019.02.002.

References

Al-Alili, A., Hwang, Y., Radermacher, R., 2014. A hybrid solar air conditioner: experimental investigation. Int. J. Refrig. 39, 117–124.
Angeline, P.J., Saunders, G.M., Pollack, J.B., 1994. An evolutionary algorithm that constructs recurrent neural networks. IEEE Trans. Neural Netw. 5 (1), 54–65.
Angrisani, G., Minichiello, F., Roselli, C., Sasso, M., 2012. Experimental analysis on the dehumidification and thermal performance of a desiccant wheel. Appl. Energy 92, 563–572.
ASHRAE, 2007. Standard, method of testing for rating desiccant dehumidifiers utilizing heat for the regeneration process.
Beccali, M., Butera, F., Guanella, R., Adhikari, R., 2003. Simplified models for the performance evaluation of desiccant wheel dehumidification. Int. J. Energy Res. 27 (1), 17–29.
Bengio, Y., Courville, A., Vincent, P., 2013. Representation learning: a review and new perspectives. IEEE Trans. Pattern Anal. Mach. Intell. 35 (8), 1798–1828.
Bishop, C.M., 1995. Neural Networks for Pattern Recognition. Oxford University Press.

Bornehag, C.-G., Blomquist, G., Gyntelberg, F., Järvholm, B., Malmberg, P., Nordvall, L., Nielsen, A., Pershagen, G., Sundell, J., 2001. Dampness in buildings and health. nordic interdisciplinary review of the scientific evidence on associations between exposure to “dampness” in buildings and health effects (NORDDAMP). Indoor Air 11 (2), 72–86.

Cao, T., Lee, H., Hwang, Y., Radermacher, R., Chun, H.-H., 2014. Experimental investigations on thin polymer desiccant wheel performance. Int. J. Refrig. 44, 1–11.

Comino, F., de Adana, M.R., Peci, F., 2016. First and second order simplified models for the performance evaluation of low temperature activated desiccant wheels. Energy Build. 116, 574–582.

De Antonellis, S., Intini, M., Joppolo, C.M., Romano, F., 2016. On the control of desiccant wheels in low temperature drying processes. Int. J. Refrig. 70, 171–182.

De Antonellis, S., Kim, D.-S., 2018. Effectiveness of a symmetric desiccant wheel operating in balanced flow condition: modeling and application. Int. J. Refrig. 88, 347–359.

Durbin, R., Rumelhart, D.E., 1989. Product units: a computationally powerful and biologically plausible extension to backpropagation networks. Neural Comput. 1 (1), 133–142.

Harriman III, L., Brundrett, G.K.R., 2001. Humidity control design guide. Technical Report. American Society of Heating, Refrigerating, and Air Conditioning Engineers, Inc. (ASHRAE), 1791 Tullie Circle, N.E., Atlante, GA 30329.

Haykin, S.S., 2009. Neural networks and learning machines, 3. Pearson Upper Saddle River, NJ, USA:.

Hornik, K., Stinchcombe, M., White, H., 1989. Multilayer feedforward networks are universal approximators. Neural Netw. 2 (5), 359–366.

Jani, D., Mishra, M., Sahoo, P., 2016. Performance prediction of rotary solid desiccant dehumidifier in hybrid air-conditioning system using artificial neural network. Appl. Thermal Eng. 98, 1091–1103.

Jani, D., Mishra, M., Sahoo, P., 2017. Application of artificial neural network for predicting performance of solid desiccant cooling systems–a review. Renew. Sustain. Energy Rev. 80, 352–366.

Koronaki, I., Rogdakis, E., Kakatsiou, T., 2012. Thermodynamic analysis of an open cycle solid desiccant cooling system using artificial neural network. Energy Convers. Manag. 60, 152–160.

Kosar, D., 2006. Dehumidification system enhancements. ASHRAE J. 48 (2), 48.

Maclaine-Cross, I., Banks, P., 1972. Coupled heat and mass transfer in regenerator-spreduction using an analogy with heat transfer. Int. J. Heat Mass Transf. 15 (6), 1225–1242.

Martínez-Estudillo, A., Martínez-Estudillo, F., Hervás-Martínez, C., García-Pedrajas, N., 2006. Evolutionary product unit based neural networks for regression. Neural Netw. 19 (4), 477–486.

Mazzei, P., Minichiello, F., Palma, D., 2005. HVAC dehumidification systems for thermal comfort: a critical review. Appl. Thermal Eng. 25 (5–6), 677–707.

Mohammad, A.T., Mat, S.B., Sulaiman, M., Sopian, K., Al-Abidi, A.A., 2013. Artificial neural network analysis of liquid desiccant regenerator performance in a solar hybrid air-conditioning system. Sustain. Energy Technol. Assess. 4, 11–19.

Parmar, H., Hindoliya, D., 2011. Artificial neural network based modelling of desiccant wheel. Energy Build. 43 (12), 3505–3513.

Ruivo, C., Carrillo-Andrés, A., Costa, J., Domínguez-Muñoz, F., 2013. A new approach to the effectiveness method for the simulation of desiccant wheels with variable inlet states and airflows rates. Appl. Thermal Eng. 58 (1–2), 670–678.

Ruivo, C., Costa, J., Figueiredo, A., 2007. On the behaviour of hygroscopic wheels: part I–channel modelling. Int. J. Heat Mass Transf. 50 (23–24), 4812–4822.

Uçkan, İ., Yılmaz, T., Hürdoğan, E., Büyükalaca, O., 2015. Development of an artificial neural network model for the prediction of the performance of a silica-gel desiccant wheel. Int. J. Green Energy 12 (11), 1159–1168.

Wang, J., Brown, C., Cleland, D., 2018. Heat pump heat recovery options for food industry dryers. Int. J. Refrig. 86, 48–55.

White, S.D., Goldsworthy, M., Reece, R., Spillmann, T., Gorur, A., Lee, D.-Y., 2011. Characterization of desiccant wheels with alternative materials at low regeneration temperatures. Int. J. Refrig. 34 (8), 1786–1791.

Yang, Y., Cong, H., Jiang, P., Feng, F., Zhang, P., Li, Y., Hao, J., 2017. Desiccant wheel system modeling improvement using multiple population genetic algorithm training of neural network. Dry. Technol. 35 (14), 1663–1674.

Zain, A.M., Haron, H., Sharif, S., 2010. Prediction of surface roughness in the end milling machining using artificial neural network. Expert Syst. Appl. 37 (2), 1755–1768.

Zendehboudi, A., Li, X., 2018. Desiccant-wheel optimization via response surface methodology and multi-objective genetic algorithm. Energy Convers. Manag. 174, 649–660.